Journal of Materials Chemistry B

Accepted Manuscript

ROYAL SOCIETY OF CHEMISTRY

www.rsc.org/materialsB

Journal Name

ARTICLE

The preparation, drug loading and in-vitro NIR photothermal-controlled release behavior of raspberry-like hollow polypyrrole microspheres

[1]Received 00th January 20xx,
Accepted 00th January 20xx

DOI: 10.1039/x0xx00000x

www.rsc.org/

Jie Wang, Fuxing Lin, Jinxing Chen, Mozhen Wang, and Xuewu Ge*

The combination of NIR photothermal therapy and chemotherapy is considered as the promising technique for the future cancer therapy. The key point for this technique is the design and synthesis of photothermal agents with high-efficiency phtotothermal effect and high chemical drug loading capacity. Herein, submicron-sized raspberry-like hollow-structured polypyrrole microspheres (H-PPy) were facily prepared through the in-situ polymerization of pyrrole on monodispersed polystyrene (PS) template microspheres with a diameter of 220 nm, followed by the chemical etching of the PS templates. The prepared H-PPy microspheres show rapid and remarkable photothermal effect in water under the irradiation of NIR laser (808 nm) only for 5 min. Further, a model small molecular drug, (S)-(+)-camptothecin (CPT), were loaded into the void core by a simple dispersion-permeation process through the micro-pores on the raspberry-like PPy shell, with a load capacity of 0.14 mg/(mg H-PPy). The MTT assay and the in vitro NIR-laser triggered release behavior indicated that the pure H-PPy microspheres have good biosafety, but the release of loaded CPT in H-PPy microsphere can be achieved with remarkable spatial/temporal resolution after NIR laser irradiation, which results in the excellent synergistic effect of photothermal and chemical ablation on HeLa cells, as proved by the fluorescence microscopy. This work provides a convenient synthesis of a promising cancer therapy agent with high drug-loading capacity and efficient NIR light photothermal effect, which can perfectly achieve the synergistic NIR photothermal therapy and chemotherapy of PPy microspheres.

Introduction

The photothermal agents which exhibit strong photothermal effect under the irradiation of near-infrared light (NIR, λ = 700 - 1200 nm) have attracted much attention in the field of biology during the last few years.[1-6] Some of them have shown encouraging application prospect in the photothermal ablation of cancer cells because NIR laser has a deeper tissue penetration and minimal tissue invasion, as well as an excellent spatial/temporal resolution in biological tissues.[7-11] Various inorganic nanomaterials, such as gold with various nanostructures,[12-15] carbon nanomaterials,[16-18] copper-based nanocrystals,[19-21] WS_2 nanosheets[22], MoS_2 nanosheets,[23] and WO_{3-x} nanoparticles,[24] have been found to show available photothermal effect to kill cancer cells. However, their low photostability and potential long-term toxicity limit their widespread application.[25,26] In contrast, polymeric materials are considered to be promising ideal photothermal agents due to their effective photostability, excellent biocompatibility and outstanding biodegradability.[27,28] For example, in vitro and in vivo experiments have indicated that polypyrrole (PPy) and its composites exhibit excellent photothermal conversion efficiency and very low long-term cytotoxicity so as to have outstanding therapeutic effect in shallow-located tumors.[29-34] At the same time, the light absorption of PPy microspheres is very stable, and won't be affected by long-time irradiation and environmental pH.[26,35] But for the ablation of deep-located tumors, using the photothermal agents alone is not enough due to the unavoidable depth-dependent attenuation of laser intensity.[36,37] Therefore, the integration of photothermal ablation and chemotherapy in one system becomes a hot spot in the photothermic therapy.[38] Liu et al. prepared a NIR-laser triggered multifunctional drug delivery platform based on PPy-coated magnetic nanoparticles, on which the drug molecules with aromatic structures (e.g. DOX) can be loaded.[39] The PPy shell exhibited a strong photothermal effect, which enhanced the chemotherapeutic efficacy, showing an outstanding in vivo synergistic antitumor effect. However, the loading of drug molecules only based on the physical adsorption on a surface layer has some disadvantages, such as limited loading capacity and easy molecule losing during the transferring process, causing several side effects. Therefore, the synthesis of drug delivery carrier with high loading capacity and stability is necessary. But till now, the design and synthesis of such high

CAS Key Laboratory of Soft Matter Chemistry, Department of Polymer Science and Engineering, University of Science and Technology of China, Hefei, Anhui 230026, P. R. China
** To whom correspondence should be addressed. E-mail: xwge@ustc.edu.cn; Tel: +86-551-63600843*
† Footnotes relating to the title and/or authors should appear here.
Electronic Supplementary Information (ESI) available: [details of any supplementary information available should be included here]. See DOI: 10.1039/x0xx00000x

efficient polymer microspheres which integrate chemotherapeutic drugs and photothermal agents into one system is still a challenge.

Herein, we prepared a raspberry-like hollow polypyrrole (H-PPy) microspheres with a size of about 220 nm by a sacrificial template method. A model small molecular drug, (S)-(+)-camptothecin (CPT), can be easily loaded into the void core through the micro-pores on the raspberry-like PPy shell. The hollow core of the H-PPy microspheres provides a high loading capacity, and the PPy shell can act as a gatekeeper to prevent the drug from escaping. The H-PPy microspheres show low cytotoxicity, excellent photostability, and outstanding photothermal conversion efficiency, which enables the NIR-laser triggered release of the loaded CPT molecules. Thus the CPT-loaded H-PPy microspheres show strong power to kill HeLa cells under the irradiation of NIR laser. This work provides a potential application prospect for the efficient synergistic NIR photothermal therapy and chemotherapy of PPy microspheres.

Experimental

Reagents and materials

Potassium persulfate (KPS, 98%) was recrystallized by deionized water before used. Styrene (St, 99%) was distilled under vacuum. Pyrrole (98%), tetrahydrofuran (THF, 99%), dimethylsulfoxide (DMSO, 99%), ethanol (99.7%), ammonium persulfate ($(NH_4)_2S_2O_8$, 98%), polyvinylpyrrolidone (PVP, K30, 97%), and concentrated hydrochloric acid (36% ~ 38%) were all purchased from Shanghai Chemical Reagents Corporation, and used without further purification. Fetal bovine serum (FBS), trypsin and Dulbecco's modified Eagle's medium (DMEM) were obtained from GIBCO, and used as received. (S)-(+)-Camptothecin (CPT, ≥ 90%), 3-(4,5-dimethylthiazol-2-yl)-2,5-diphenyltetrazolium bromide (MTT, 98%), 5-carboxyfluorescein diacetate (5-CFDA), and propidium iodide (PI) were purchased from Sigma-Aldrich, and used as received.

Synthesis of monodispersed polystyrene (PS) microspheres

Styrene (11 mL) was added into 90 mL of deionized water, in which 2 g of PVP was dissolved. The mixture was degassed with bubbling N_2, and heated to 70 °C in an oil bath under mechanical agitation (250 rpm). Then, an aqueous solution (1 mL) containing 0.1 g of KPS was dropped in to initiate the polymerization of styrene. The polymerization reaction was carried out for 24 h. The produced PS microspheres were separated by centrifugation at 15000 rpm for 20 min, and washed with deionized water and ethanol respectively for three times.

Synthesis of hollow polypyrrole (H-PPy) microspheres

The as-prepared PS microspheres (0.1 g) were dispersed ultrasonically in 100 mL of deionized water. Then a solution of 0.1 mL of pyrrole and 2.5 mL of ethanol was dropped into the above aqueous dispersion under magnetic stirring. Then, the system was put in an ice bath, and 9 mL of concentrated hydrochloric acid was added in. After the system was continuously stirred magnetically for 2 h, an aqueous solution of $(NH_4)_2S_2O_8$ (5 mL, 20 mg/mL) was added to initiate the polymerization reaction of pyrrole. The polymerization reaction lasted for 6 h. The products, termed as PS@PPy microspheres, were centrifugated, and washed with deionized water and ethanol respectively for 3 times. After being dried in vacuum at 50 °C for 24 h, the PS@PPy microspheres were dispersed in 25 mL of tetrahydrofuran (THF). The dispersion was put in an oil bath at 40 °C, and magnetically stirred for 8 h to remove PS microspheres. The final products, named as H-PPy, were centrifugated, washed with deionized water and ethanol respectively for 3 times, and freeze-dried.

Morphological characterization

The morphologies of PS microspheres, PS@PPy microspheres, and H-PPy microspheres were observed with scanning electron microscope (SEM) (JEOL JSM6700, 5 kV) and transmission electron microscopy (TEM) (Hitachi H7650, 100 kV).Samples were prepared by dispersing a small drop of the ethanol dispersion of the sample onto copper grids. The samples for SEM observation were treated by spray-gold.

N_2 adsorption-desorption isotherms of the prepared microspheres were conducted on a Micromeritics Tristar II 3020 V1.03 analyzer after the samples were outgassed at 100 °C for 5 h. The specific surface area and pore size distribution were analyzed by Brunauer–Emmett–Teller (BET) and Barret–Joyner–Halenda (BJH) methods, respectively. The total pore volume of the samples was calculated at P/P_0= 0.97. Fourier transform infrared (FTIR) spectra were recorded in the range from 4000 to 400 cm^{-1} with a Bruker VECTOR-22 IR spectrometer using KBr pellets. Dynamic light scattering analysis (DLS) were conducted on a Malvern Zetasizer Nano ZS-2S90 instrument using a deionized water dispersion of the sample.

Measurement of the photothermal performance of H-PPy microspheres

The light absorption of H-PPy microspheres was analyzed by the Ultraviolet–visible–near-infrared (UV-Vis-NIR) absorption spectrum recorded by Shimadzu spectrophotometer (UV-3600).

The photothermal performance of H-PPy microsphere in the aqueous solution was measured on an 808 nm semiconductor laser device (ADR-1860, China) with externally adjustable power. The irradiation time was fixed to 5 min in all the experiments. An online thermocouple (TP-01, Taiwan) with an accuracy of 0.1 °C was immersed into the solution to record the temperature once a second.

CPT loading into H-PPy microspheres

H-PPy microspheres (24 mg) were dispersed into the DMSO solution of CPT (6 mL, 2 mg/mL). The mixture was magnetically stirred in darkness at room temperature for 3 days to reach the equilibrium state. The CPT-loaded H-PPy microspheres were obtained by centrifugation at 10000 rpm for 6 min. The

CPT-loaded H-PPy microspheres were dried under vacuum. The loading capacity of CPT into H-PPy microspheres (L_{CPT}) was determined by the following Equation 1:

$$L_{CPT} = \frac{m_0 - c_e \times V}{M} \text{(mg/mg microsphere)} \quad (1)$$

Here, m_0 is the original mass of CPT added in the solution, i.e., 12 mg; c_e is the concentration of CPT in the solution at a unit of mg/mL after the adsorption of CPT in H-PPy microspheres reached the equilibrium state, which was measured by UV-vis spectroscopy (Shimadzu spectrophotometer, UV-2401PC) at the wavelength of 366 nm. V is the volume of the adsorption solution, i.e. 6 mL. M is the mass of the total H-PPy microspheres added in the adsorption solution, i.e. 24 mg.

The NIR-laser triggered release behavior of CPT loaded in H-PPy microspheres

The NIR-laser triggered drug release experiments were performed in 5 mL of DMSO aqueous solution (5% v/v), which contained 0.4 mg of CPT-loaded H-PPy microspheres. For each cycle, the suspension was first irradiated for 5 min at a power density of 3.3 W/cm^2, then the laser source was power off. After 10 min, the suspension were sampled and centrifuged at 10000 rpm for 6 min to measure the amount of the released CPT by UV-vis.

As a control, the release curve of CPT-loaded H-PPy microspheres in the same solvent without laser irradiation were also recorded.

Cytotoxicity assay

The toxicity of H-PPy microspheres to cells was evaluated by MTT assay. HeLa cells were cultured in Dulbecco's Modified Eagle Medium (DMEM) supplemented with 10% (v/v) fetal bovine serum. The cells were cultured in 96-well plates at a density of 5,000 cells/well and incubated at 37 °C in 5% CO_2 for 24 h. Then, the culture medium was changed and cells were incubated with fresh medium containing the H-PPy microspheres with different concentrations (10, 20, 40, 60, 80, and 100 μg/mL) for 24 h. After that, 20 μL of MTT solution (5 mg/mL) was added to each well, and then was incubated for another 4 h. The MTT solution was removed, and 150 μL of DMSO was added to each well to dissolve the the formazan crystals. The plates were shaken for 15 min to ensure formazan crystals to be dissolved completely. Finally, the absorbance was measured by microplate reader (Thermo Fisher, USA) at 490 nm. Five replicates were done for each treatment group.

Investigation on the in vitro therapeutic effect of the CPT loaded H-PPy microspheres

HeLa cells were cultured in 96-well plates and incubated at 37 °C in 5% CO_2 for 24 h. Then, the culture medium was replaced by the fresh culture medium which respectively contains PBS, free CPT (5 μg/mL), H-PPy microspheres (35 μg/mL), and CPT-loaded H-PPy microspheres (40 μg/mL). After 4 h, excess CPT or H-PPy microspheres were removed by washing with PBS for three times. Fresh culture medium was added to the wells again. Then, the cells were irradiated by NIR laser (3.3 W/cm^2) for 5 min, and incubated again at 37 °C with 5% CO_2 for 24 h. 20 μL of MTT solution (5 mg/mL) was added to each well of the plate, and then was incubated for 4 h. The MTT solution was suctioned, and 150 μL of DMSO was added to each well to dissolve the formazan crystals. The plates were shaken for 15 min to ensure formazan crystals to be dissolved completely. Finally, the absorbance was measured by microplate reader at 490 nm. Five replicates were done for each treatment group.

The in vitro therapeutic effect of the samples was also studied by the fluorescence imaging. The pre-treatment of the cells was the same with the above MTT assay. The difference is that the cells were incubated at 37 °C with 5% CO_2 for only 2 h after being irradiated by NIR laser (3.3 W/cm^2) for 5 min. After washed with PBS, the cells were co-stained by 5-CFDA (2 μM) and PI (4 μM). Finally, the fluorescence imaging of the cells were conducted on fluorescence microscope (OLYMPUS IX71).

Results and Discussion

Preparation, morphology, and photothermal effect of the raspberry-like H-PPy microspheres

Templating method is often used to produce hollow spheres.[40] It is well-known that PPy nanoparticles can be readily synthesized in water at room temperature using chemical oxidants such as $FeCl_3$ or $(NH_4)S_2O_8$,[41-43] and PPy is preferentially deposited onto hydrophobic substrates.[44] Therefore, the preparation of raspberry-like H-PPy microspheres in this work can be achieved by in-situ formation of PPy nanoparticles around on the polymer microspheres, followed by removing the polymer microspheres, as illustrated in Figure 1. Firstly, monodispersed PS microspheres with an average diameter of 216 nm, as shown in Figure 1a and 1a', were synthesized through an emulsion polymerization of styrene stabilized by PVP.[45] The size distribution and the zeta potential of PS microspheres also had been measured by DLS (see Figure S1). The Z-average size is 225 nm, a little bit larger than that measured from SEM images, since the size measured from DLS is the hydraulic diameter of the particles. The zeta potential of PS microspheres is –21 mV, which means the surface of PS microspheres is negative charged. Next, the prepared negatively charged PS microspheres were dispersed into the acidic aqueous solution of pyrrole. Since pyrrole monomer will be positive charged in the acidic polymerization conditions, pyrrole will be tend to be adsorbed onto the surface of PS microspheres.[46] As a result, pyrrole monomers polymerized to form nanoparticles, resulting in the formation of a raspberry-like particulate PPy shell on PS microspheres. Figure 1b and 1b' clearly exhibit the morphology of the raspberry-like core-shell structured PS@PPy microspheres with a larger average diameter of 240 nm. Finally, the prepared PS@PPy microspheres were immersed into THF to etch the PS core, and H-PPy microspheres were obtained, as shown in

Figure 1c and 1c'. The H-PPy microspheres remain the raspberry-like shape. Compared with Figure 1b' and 1c', the hollow structure of H-PPy microspheres can be confirmed. The PPy particulate shell has a thickness of about 30 nm. The DLS result in Figure S1 also shows the H-PPy microspheres have a Z-average size of 358 nm and a narrow size distribution, i.e., PDI is 0.116. The same narrow size distribution between PS and H-PPy microspheres proves that PPy nanoparticles are in-situ formed homogeneously on the surface of PS microspheres.

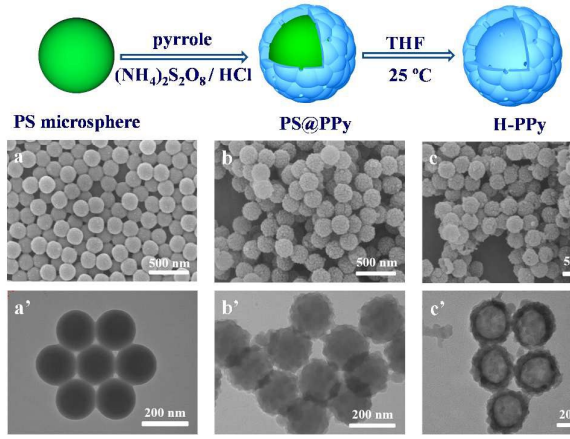

Figure 1. Schematic illustration of the synthesis of H-PPy microspheres. The SEM and TEM images of PS microspheres (a, a'), PS@PPy microspheres (b, b'), and H-PPy microspheres (c, c').

The FTIR spectrum of H-PPy microspheres is shown in Figure 2, together with those of PS and PS@PPy microspheres. The well-known characteristic symmetry and asymmetric stretching vibration peaks of pyrrole ring located at 1552 and 1449 cm^{-1}, as well as the peak assigned to the C–N stretching vibration at 1176 cm^{-1}, can be clearly seen on the FTIR spectrum of H-PPy.[44, 47, 48] At the same time, the characteristic stretching vibration peaks of the aromatic rings at 1400-1500 cm^{-1} and the aliphatic C–H stretching vibration centred at 2848 and 2967 cm^{-1} on PS molecular chains nearly cannot be detected, although they all can be observed on the FTIR spectra of PS and PS@PPy microspheres. The above results also indicate the formation of the hollow PPy structure.

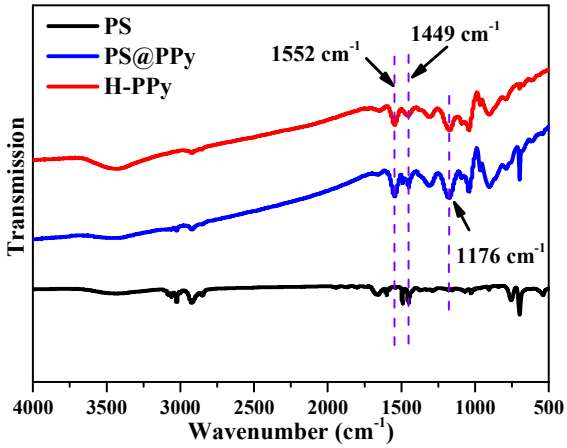

Figure 2. FTIR spectra of PS, PS@PPy, and H-PPy microspheres

The N_2 adsorption-desorption isotherms of H-PPy microspheres are displayed in Figure 3. It indicates a typical type II N_2 adsorption-desorption isotherms according to BDDT classification.[49] There is nearly no hysteresis during the desorption process, which means almost no existence of mesopores. However, the rapid increase of the adsorption observed when P/P_0 is above 0.9 implies the presence of macropores. The pore size distribution curve also indicates a microporous and macroporous structure of H-PPy. This result is in accord with the morphology of H-PPy observed by TEM. The BET surface area and total pore volume calculated by BJH method are 66.2 $m^2.g^{-1}$ and 0.18 $cm^3.g^{-1}$, respectively.

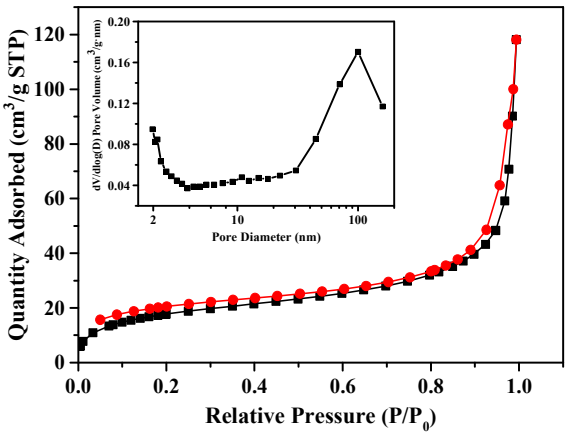

Figure 3. The N_2 adsorption-desorption isotherms of H-PPy microspheres. The inset is the BJH pore-diameter distribution.

The UV-vis-NIR spectrum of H-PPy microspheres in Figure 4a shows that H-PPy has a strong absorption of NIR light (800 – 1200 nm), which is in accord with the NIR absorption of polypyrrole and its composites reported in literatures.[50] Thus, a 808 nm NIR laser was chosen in this work as the light source to investigate the photothermal conversion performance of H-

PPy microspheres. Figure 4b records the temperature change of the aqueous dispersion containing a certain amount of H-PPy microspheres (0.01 mg/mL) within 5-min's irradiation of 808 nm laser with a different power density. It is seen that an obvious increase of the temperature when the laser power density reaches 3.3 W/cm^2, which indicates the prepared H-PPy microspheres show a good photothermal effect. Moreover, the larger the laser power density, the higher temperature the dispersion increases to, i.e., the stronger the photothermal effect, within the same time. Considering the application of NIR photothermal effect of H-PPy microspheres on the living cells, a low laser power density of 3.3 W/cm^2 is adopted all through the following work to ensure the living cells won't be killed by the laser irradiation with a large power density. Figure 4c shows the temperature changes of the aqueous dispersion containing different content of H-PPy microspheres within 5-min's irradiation of NIR laser (808 nm, 3.3 W/cm^2). The photothermal effect of H-PPy microspheres is enhanced with the increase of their content in water. On the contrary, the temperature change of the pure water is almost negligible, i.e., doesn't exceed 3 °C. Therefore, it can be concluded that the H-PPy microspheres can convert the absorbed photon energy into heat rapidly and efficiently. At the same time, the photothermal performance can remain without any loss after at least five cycles, as shown in Figure 4d. Moreover, the H-PPy microspheres have great photostability for the long-time irradiation of NIR light because there appears no change on the morphology of the microspheres before and after the five-circles' irradiation of NIR light (Figure 4d, inset TEM images), unlike some other nano-metal photothermal agents, such as Au nanorods, which would "melt" and lose their NIR absorbance after a long period of NIR laser irradiation.[26] Therefore, it can be concluded that H-PPy microspheres can be used as an ideal photothermal agent in cancer therapy.

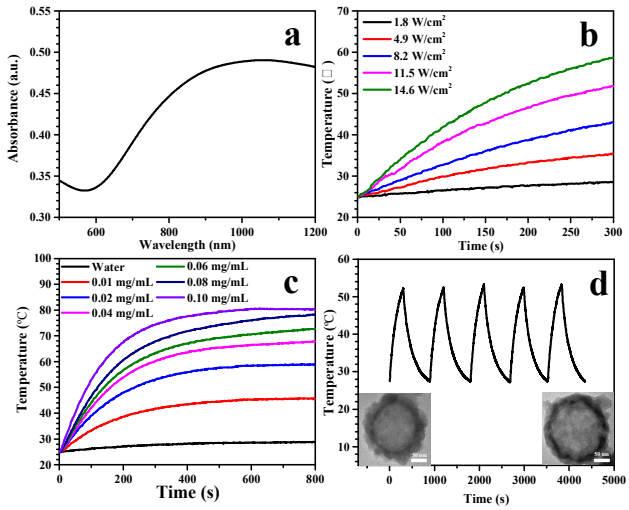

Figure 4. (a) UV-vis-NIR absorption spectrum of the aqueous dispersion of H-PPy microspheres; (b) The curves of temperature v.s. irradiation time of the aqueous dispersion of H-PPy microspheres (0.01 mg/mL) irradiated by 808 nm laser with different power density; (c) The curves of temperature v.s. irradiation time of the aqueous dispersion containing different content of H-PPy microspheres irradiated by NIR laser (808 nm, 3.3 W/cm^2); (d) Temperature variation of the aqueous dispersion of H-PPy microspheres (0.06 mg/mL) over five laser irradiation ON/OFF cycles (808 nm, 3.3 W/cm^2). The insets are the TEM images of the H-PPy microspheres before and after five-cycle's irradiation.

The loading and NIR-laser triggered release behavior of CPT in H-PPy microspheres

(S)-(+)-Camptothecin (CPT) is a well-known small molecular drug for its wide clinical application in cancer therapy. But its power to kill cancer cells is limited by its poor water-solubility and cellular uptake efficiency. Herein, CPT can be firstly loaded in the cavity of H-PPy microspheres by a common diffusion and permeation method based on the micro-/macro-porous structure of H-PPy microspheres, and then release on demand triggered by the irradiation of NIR laser due to the remarkable photothermal effect of the H-PPy microspheres, as illustrated in Figure 5. Figure S1(c) proves that there are slight changes in the size distribution and zeta potential of H-PPy microspheres after the loading of CPT. The load capacity of CPT can reach 0.14 mg/(mg H-PPy). The cumulative release profiles of CPT from H-PPy microspheres dispersed in the aqueous solution of DMSO (5% v/v) within 48 h at 25 °C and 45 °C are studied to make sure whether CPT can release rapidly at a relative high temperature, as shown in Figure 5a. Evidently, a burst release of CPT occurs at 45 °C, compared with that at 25 °C. 40% of the loaded CPT will be released within 5 h, 4 times the release amount at 25 °C. The maximum release amount of CPT within 48 h at 45 °C can achieve 70%, also much higher than that at 25 °C (30%).

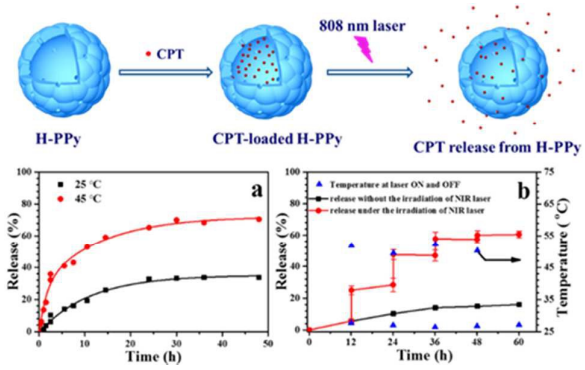

Figure 5. Schematic illustration of the loading and NIR-laser-triggered release of camptothecin (CPT) in H-PPy microspheres. (a) The release profiles of CPT from H-PPy microspheres dispersed in the aqueous solution of DMSO (5% v/v) at 25 °C and 45 °C; (b) The release profile of CPT from H-PPy microspheres dispersed in the aqueous solution of DMSO (5% v/v) (0.1 mg/mL) under the irradiation of NIR laser (808 nm, 3.3 W/cm^2) for 5 min with a ON/OFF-mode every 12 h (-•-, Left Ordinate), and the corresponding temperature of the dispersion at every ON and OFF point (▲, Right Ordinate). As a control, the release profile of CPT in the same dispersion without the irradiation of NIR laser is also listed (-▪-, Left Ordinate).

The NIR-laser triggered release behavior of CPT in the same solvent is recorded in Figure 5b. Here, the NIR laser trigger was operated by laser ON for 5 min then laser OFF, i.e., a laser

ON/OFF mode. This trigger operation was repeated every 12 h. Both the accumulative release ratio of CPT and the temperature of the H-PPy dispersion were recorded at every laser ON and OFF points. During the first 24 h, a burst release of CPT (about a 20% of release ratio) can be detected at every laser OFF point, along with a temperature increase of about 25 degree of the H-PPy dispersion. Then, the release of CPT slows down, till level off after 48 h. The total release ratio within 60 h reach 60%. As a comparison, the total release of CPT in the H-PPy dispersion without any irradiation of NIR laser within the same time doesn't exceed 17%. The results confirm that the photothermal effect of H-PPy microspheres is enough efficient to be used in the controlled drug release stimulated by NIR laser irradiation.

The in-vitro photothermal ablation of HeLa cells using CPT loaded H-PPy microspheres

The cell toxicity of H-PPy microspheres was evaluated by MMT assay on HeLa cells, as shown in Figure 6a. It proves that H-PPy microspheres have good in vitro biosecurity at a content ranging from 10 to 100 μg/mL. The NIR laser of 808 nm is also safe to HeLa cells basically, referring to the cell viability in Figure 6b (NIR laser). However, the cell viability will decrease to 57% if HeLa cells are incubated in DMEM medium containing H-PPy microsphere and irradiated by NIR laser (see Figure 6b (H-PPy/NIR laser)), even lower than that incubated at the present of CPT (76%, Figure 6b (CPT)) and CPT-loaded H-PPy microspheres (62%, Figure 6b (H-PPy+CPT)). It indicates that the photothermal effect of H-PPy microspheres has a better power to kill HeLa cells in DEME medium than pure CPT or CPT-loaded H-PPy microspheres which should be caused by the poor solubility and the low uptake of CPT. The cell viability will further decrease to 42% if HeLa cells are incubated in DMEM medium containing both H-PPy microsphere and CPT, and then irradiated by NIR laser (see Figure 6b (H-PPy/CPT/NIR laser). However, it is so exciting that the cell viability falls straight down to only 20% when HeLa cell is incubated at the presence of CPT-loaded H-PPy microspheres along with 5-min's NIR laser irradiation (Figure 6b (H-PPy+CPT/NIR laser)), which means a synergistic enhancement on the ability to kill HeLa cells attributed to photothermal ablation of H-PPy microspheres and the chemical ablation of CPT released from H-PPy microspheres triggered by the irradiation of NIR laser.

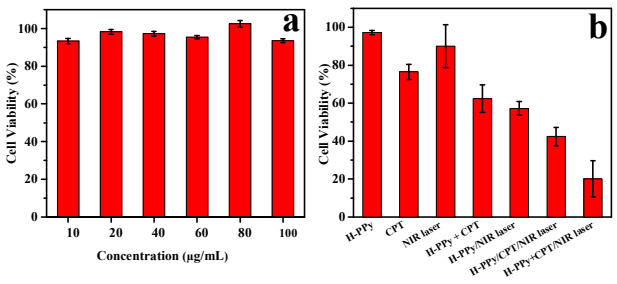

Figure 6. (a) The cell viability of HeLa cells after being incubated in DMEM medium with different content of H-PPy microspheres for 24 h. (b) The cell viability of HeLa cells after being incubated in DMEM medium containing different active species: i) 35 μg/mL of H-PPy microspheres (H-PPy), ii) 5 μg/mL of pure CPT (CPT), iii) pure DMEM under the irradiation of NIR laser (NIR laser), iv) 40 μg/mL of CPT-loaded H-PPy microspheres (H-PPy+CPT), v) 35 μg /mL of H-PPy microspheres under the irradiation of NIR laser (H-PPy/NIR laser), vi) 35 μg/mL of H-PPy microspheres and 5 μg/mL of pure CPT under the irradiation of NIR laser (H-PPy/CPT/NIR laser), and vii) 40 μg/mL of CPT-loaded H-PPy microspheres under the irradiation of NIR laser (H-PPy+CPT/NIR laser). The conditions of the NIR laser irradiation: 808 nm, 3.3 W/cm^2, for 5 min.

To further validate the synergistic photothermal and chemical ablation effect of CPT-loaded microspheres, the HeLa cells were co-stained by 5-carboxyfluorescein diacetate (5-CFDA) and propidium iodide (PI) to differentiate live (green) and dead (red) cells respectively, as shown in Figure 7. It is obviously discovered that HeLa cells are efficiently killed only when they are treated with CPT-loaded H-PPy microsphere under the irradiation of NIR laser (Figure 7f). For comparison, H-PPy microspheres, free CPT and CPT-loaded H-PPy microspheres without any irradiation of NIR laser can only show a moderate or negligible power to kill HeLa cells (Figure 7b – 7d), as well as the case of the unloaded H-PPy microspheres under the irradiation of NIR laser (Figure 7e). The results are in accord with the MTT assay in Figure 6, which confirms the synergistic photothermal and chemical ablation effect of CPT-loaded microspheres.

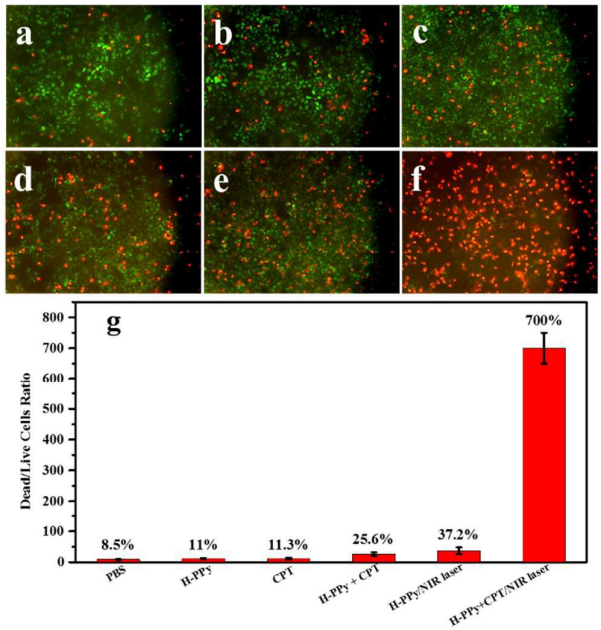

Figure 7. The fluorescence microscopy images of HeLa cells treated with a) PBS. b) H-PPy microspheres (35 μg/mL). c) free CPT (5 μg/mL). d) CPT-loaded H-PPy microspheres (40 μg/mL). e) H-PPy microspheres (35 μg/mL) under the irradiation of NIR laser. f) CPT-loaded H-PPy microspheres (40 μg/mL) under the irradiation of NIR laser. Viable cells were stained green with 5-CFDA, dead cells were stained red with PI. The conditions of the NIR laser irradiation: 808 nm, 3.3 W/cm^2, for 5 min. g) The dead/live ratio of HeLa cells of a) – f).

Conclusions

In this work, monodispersed raspberry-like hollow-structured PPy microspheres (H-PPy) with an average size of 220 nm were successfully prepared through the in-situ growth of PPy nanoparticles on PS template microspheres, followed by the etching of PS template with THF. When the H-PPy microspheres were dispersed in aqueous solution and irradiated by NIR laser (808 nm), they showed significant photothermal conversion effect, and also had excellent photostability. CPT can be conveniently loaded through a simple dispersion-permeation method, with a load capacity of 0.14 mg/(mg H-PPy). The MTT assay and the in vitro NIR-laser triggered release behavior indicated that the pure H-PPy microspheres have good biosafety, but the release of loaded CPT in H-PPy microsphere can be achieved with remarkable spatial/temporal resolution after NIR laser irradiation, which results in the excellent synergistic effect of photothermal and chemical ablation of HeLa cells. The high drug-loading capacity and efficient NIR light photothermal effect, as well as the convenient synthesis route, make the raspberry H-PPy microspheres have the potential to be used as a promising cancer therapy agent.

Acknowledgements

We thank Prof. Zhishen Ge in Department of Polymer Science and Engineering of USTC for his kind help in providing the 808 nm semiconductor laser device, and the valuable instructions for MTT assay. This work was supported by the National Natural Science Foundation of China (Nos. 51073146, 51103143, and 51173175), the Fundamental Research Funds for the Central Universities (WK2060200012; WK34500001).

Notes and references

1 Z. J. Zhang, J. Wang and C. Y. Chen, *Adv. Mater.*, 2013, **25**, 3869-3880.
2 D. Jaque, L. M. Maestro, B. D. Rosal, P. Haro-Gonzalez, A. Benayas, J. L. Plaza, E. M. Rodríguez and J. G. Solé, *Nanoscale*, 2014, **6**, 9494-9530.
3 J. Yu, X. Chu and Y. L. Hou, *Chem. Commun.*, 2014, **50**, 11614-11630.
4 R. Z. Liang, M. Wei, D. G. Evans and X. Duan, *Chem. Commun.*, 2014, **50**, 14071-14081.
5 A. P. Blum, J. K. Kammeyer, A. M. Rush, C. E. Callmann, M. E. Hahn and N. C. Gianneschi, *J. Am. Chem. Soc.*, 2015, **137**, 2140-2154.
6 W. J. Fang, J. Yang, J. W. Gong and N. F. Zheng, *Adv. Funct. Mater.*, 2012, **22**, 842-848.
7 D. Yoo, H. Jeong, S. H. Noh, J. H. Lee and J. Cheon, *Angew. Chem. Int. Ed.*, 2013, **52**, 13047-13051.
8 G. S. Song, Q. Wang, Y. Wang, G. Lv, C. Li, R. J. Zou, Z. G. Chen, Z. Y. Qin, K. K. Huo, R. G. Hu and J. Q. Hu, *Adv. Funct. Mater.*, 2013, **23**, 4281-4292.
9 K. Dong, Z. Liu, Z. H. Li, J. S. Ren and X. G. Qu, *Adv. Mater.*, 2013, **25**, 4452-4458.
10 K. Yang, H. Xu, L. Cheng, C. Y. Sun, J. Wang and Z. Liu, *Adv. Mater.*, 2012, **24**, 5586-5592.
11 J. You, R. P. Shao, X. Wei, S. Gupta and C. Li, *Small*, 2010, **6**, 1022-1031.
12 M. S. Yavuz, Y. Y. Cheng, J. Y. Chen, C. M. Cobley, Q. Zhang, M. Rycenga, J. W. Xie, C. Kim, K. H. Song, A. G. Schwartz, L. V. Wang and Y. N. Xia, *Nat. Mater.*, 2009, **8**, 935-939.
13 R. Huschka, J. Zuloaga, M. W. Knight, L. V. Brown, P. Nordlander and N. J. Halas, *J. Am. Chem. Soc.*, 2011, **133**, 12247-12255.
14 J. You, G. D. Zhang and C. Li, *ACS Nano*, 2010, **4**, 1033-1041.
15 L. M. Wang, X. Y. Lin, J. Wang, Z. J. Hu, Y. L. Ji, S. Hou, Y. L. Zhao, X. C. Wu and C. Y. Chen, *Adv. Funct. Mater.*, 2014, **24**, 4229-4239.
16 Y. W. Chen, P. J. Chen, S. H. Hu, I. W. Chen and S. Y. Chen, *Adv. Funct. Mater.*, 2014, **24**, 451-459.
17 L. Meng, R. Chen, A. H. Jiang, L. M. Wang, P. Wang, C. Z. Li, R. Bai, Y. L. Zhao, H. Autrup and C. Y. Chen, *Small*, 2013, **9**, 1786-1798.
18 V. Krishna, A. Singh, P. Sharma, N. Iwakuma, Q. Wang, Q. Z. Zhang, J. Knapik, H. B. Jiang, S. R. Grobmyer, B. Koopman and B. Moudgil, *Small*, 2010, **6**, 2236-2241.
19 Q. W. Tian, F. R. Jiang, R. J. Zou, Q. Liu, Z. G. Chen, M. F. Zhu, S. Q. Yang, J. L. Wang, J. H. Wang and J. Q. Hu, *ACS Nano*, 2011, **5**, 9761-9771.
20 Q. W. Tian, M. H. Tang, Y. G. Sun, R. J. Zou, Z. G. Chen, M. F. Zhu, S. P. Yang, J. L. Wang, J. H. Wang and J. Q. Hu, *Adv. Mater.*, 2011, **23**, 3542-3547.
21 X. J. Liu, Q. Wang, C. Li, R. J. Zou, B. Li, G. S. Song, K. B. Xu, Y. Zheng and J. Q. Hu, *Nanoscale*, 2014, **6**, 4361-4370.
22 L. Cheng, J. J. Liu, X. Gu, H. Gong, X. Z. Shi, T. Liu, C. Wang, X. Y. Wang, G. Liu, H. Y. Xing, W. B. Bu, B. Q. Sun and Z. Liu, *Adv. Mater.*, 2014, **26**, 1886-1893.
23 T. Liu, C. Wang, X. Gu, H. Gong, L. Cheng, X. Z. Shi, L. Z. Feng, B. Q. Sun and Z. Liu, *Adv. Mater.*, 2014, **26**, 3433-3440.
24 J. H. Liu, J. G. Han, Z. C. Kang, R. Golamaully, N. N. Xu, H. P. Li and X. L. Han, *Nanoscale*, 2014, **6**, 5770-5776.
25 X. F. Lu, Y. Liu, X. J. Kong, P. E. Lobie, C. Y. Chen and T. Zhu, *Small*, 2013, **9**, 1654-1671.
26 Z. B. Zha, X. L. Yue, Q. S. Ren and Z. F. Dai, *Adv. Mater.*, 2013, **25**, 777-782.
27 X. J. Song, Q. Chen and Z. Liu, *Nano Res.*, 2015, **8**, 340-354.
28 L. Cheng, W. W. He, H. Gong, C. Wang, Q. Chen, Z. P. Cheng and Z. Liu, *Adv. Funct. Mater.*, 2013, **23**, 5893-5902.
29 M. Chen, X. L. Fang, S. H. Tang and N. F. Zheng, *Chem. Commun.*, 2012, 48, 8934-8936.
30 X. J. Song, H. Gong, S. N. Yin, L. Cheng, C. Wang, Z. W. Li, Y. G. Li, X. Y. Wang, G. Liu and Z. Liu, *Adv. Funct. Mater.*, 2014, **24**, 1194-1201.
31 Y. Wang, Y. Xiao and R. K. Tang, *Chem. Eur. J.*, 2014, **20**, 11826-11834.
32 Q. W. Tian, Q. Wang, K. X. Yao, B. Y. Teng, J. Z. Zhang, S. P. Yang and Y. Han, *Small*, 2014, **10**, 1063-1068.
33 X. L. Liang, Y. Y. Li, X. D. Li, L. J. Jing, Z. J. Deng, X. L. Yue, C. H. Li and Z. F. Dai, *Adv. Funct. Mater.*, 2015, **25**, 1451-1462.
34 M. Lin, C. R. Guo, J. Li, D. Zhou, K. Liu, X. Zhang, T. S. Xu, H. Zhang, L. P. Wang, B. Yang, *ACS Appl. Mater. Interfaces*, 2014, **6**, 5860-5868.
35 C. W. Hsiao, H. L. Chen, Z. X. Liao, R. Sureshbabu, H. C. Hsiao, S. J. Lin, Y. Chang and H. W. Sung, *Adv. Funct. Mater.*, 2015, **25**, 721-728.
36 C. Alvarez-Lorenzo, L. Bromberg and A. Concheiro, *Photochem. Photobiol.*, 2009, **85**, 848-860.
37 Q. F. Xiao, X. P. Zheng, W. B. Bu, W. Q. Ge, S. J. Zhang, F. Chen, H. Y. Xing, Q. G. Ren, W. P. Fan, K. P. Zhao, Y. Q. Hua and J. L. Shi, *J. Am. Chem. Soc.*, 2013, **135**, 13041-13048.
38 J. P. Yang, D. K. Shen, L. Zhou, W. Li, X. M. Li, C. Yao, R. Wang, A. M. El-Toni, F. Zhang and D. Y. Zhao, *Chem. Mater.*, 2013, **25**, 3030-3037.

39 C. Wang, H. Xu, C. Liang, Y. M. Liu, Z. W. Li, G. B. Yang, L. Cheng, Y. G. Li and Z. Liu, *ACS Nano*, 2013, **7**, 6782-6795.
40 Y. S. Li and J. L. Shi, *Adv. Mater.*, 2014, **26**, 3176-3205.
41 J. Y. Hong, H. Yoon and J. Jang, *Small*, 2010, **6**, 679-686.
42 X. Zhang, M. Lin, X. Y. Lin, C. T. Zhang, H. T. Wei, H. Zhang, B. Yang, *ACS Appl. Mater. Interfaces*, 2014, **6**, 450-458.
43 L. P. Lv, Y. Zhao, N. Vilbrandt, M. Gallei, A. Vimalanandan, M. Rohwerder, K. Landfester and D. Crespy, *J. Am. Chem. Soc.*, 2013, **135**, 14198-14205.
44 J. R. Lovett, L. A. Fielding, S. P. Armes and R. Buxton, *Adv. Funct. Mater.*, 2014, **24**, 1290-1299.
45 I. Kartsonakis, I. Daniilidis, G. Kordas, *J. Sol-Gel Sci. Technol.,* 2008, **48**, 24-31.
46 X. Zhang, X. W. Xu, T. T. Li, M. Lin, X. Y. Lin, H. Zhang, H. C. Sun, B. Yang, *ACS Appl. Mater. Interfaces*, 2014, **6**, 14552-14561.
47 S. Brunauer, L. S. Deming, W. E. Deming, and E. Teller, *J. Am. Chem. Soc.* 1940, **62**, 1723-1732.
48 X. Y. Wang, L. P. Heng, N. L. Yang, Q. Xie, and J. Zhai, *Chin. Chem. Lett.*, 2010, **21**, 884-887.
49 D. P. Dubal, S. H. Lee, J. G. Kim, and C. D. Lokhande, *J. Mater. Chem.*, 2012, **22**, 3044-3052.
50 K. M. Au, Z. H. Lu, S. J. Matcher and S. P. Armes, *Adv. Mater.*, 2011, **23**, 5792-5795.

The preparation, drug loading and in-vitro NIR photothermal-controlled release behavior of raspberry-like hollow polypyrrole microspheres

Jie Wang, Fuxing Lin, Jinxing, Chen, Mozhen Wang, and Xuewu Ge*

CAS Key Laboratory of Soft Matter Chemistry, Department of Polymer Science and Engineering, University of Science and Technology of China, Hefei, Anhui 230026, P. R. China

*To whom correspondence should be addressed.

E-mail: xwge@ustc.edu.cn Tel: 86-551-63607410

Graphic Abstract

Raspberry-like hollow polypyrrole microspheres (H-PPy), which is prepared through templating method, exhibits promising synergistic cancer therapy effect.